Check for updates

Targeted alpha therapy with the ^{224}Ra/^{212}Pb-TCMC-TP-3 dual alpha solution in a multicellular tumor spheroid model of osteosarcoma

Anna Julie Kjøl Tornes[1,2,3]*, Vilde Yuli Stenberg[1,2,3],
Roy Hartvig Larsen[2], Øyvind Sverre Bruland[3,4],
Mona-Elisabeth Revheim[3,5] and Asta Juzeniene[1,6]

[1]Department of Radiation Biology, Institute for Cancer Research, Oslo University Hospital, Oslo,
Norway, [2]ArtBio AS, Oslo, Norway, [3]Institute of Clinical Medicine, University of Oslo, Oslo, Norway,
[4]Department of Oncology, Oslo University Hospital, Oslo, Norway, [5]Division of Radiology
and Nuclear Medicine, Oslo University Hospital, Oslo, Norway, [6]Department of Physics, University
of Oslo, Oslo, Norway

Osteosarcoma patients with overt metastases at primary diagnosis have a 5-year survival rate of less than 20%. TP-3 is a murine IgG2b monoclonal antibody with high affinity for an epitope residing on the p80 osteosarcoma cell surface membrane antigen. The tumor-associated antigen p80 is overexpressed in osteosarcomas, and has very low normal tissue expression. We propose a novel dual alpha targeting solution containing two radionuclides from the same decay chain, including the bone-seeking ^{224}Ra, and cancer cell-surface seeking ^{212}Pb-TCMC-TP-3 for the treatment of osteoblastic bone cancers, circulating cancer cells and micrometastases. In this *in vitro* study, the cytotoxic effects of ^{212}Pb-TCMC-TP-3 (single alpha solution) and ^{224}Ra/^{212}Pb-TCMC-TP-3 (dual alpha solution) were investigated in a multicellular spheroid model mimicking micrometastatic disease in osteosarcoma. OHS spheroids with diameters of 253 ± 98 μm treated with 4.5, 2.7, and 3.3 kBq/ml of ^{212}Pb-TCMC-TP-3 for 1, 4, and 24 h, respectively, were disintegrated within 3 weeks. The ^{212}Pb-TCMC-TP-3 induced a 7-fold delay in spheroid doubling time compared to a 28-times higher dose with the non-specific ^{212}Pb-TCMC-rituximab. The ^{224}Ra/^{212}Pb-TCMC-TP-3 completely disintegrated spheroids with diameters of $218-476$ μm within 3 and 2 weeks after 4 and 24 h incubation with 5 kBq/ml, respectively. Treatment with 1 kBq/ml of ^{224}Ra/^{212}Pb-TCMC-TP-3 for 24 h caused an 11.4-fold reduction in spheroid viability compared with unconjugated ^{224}Ra/^{212}Pb. The

single and dual alpha solutions with TP-3 showed cytotoxicity in spheroids of clinically relevant size, which warrant further testing of the dual alpha solution using *in vivo* osteosarcoma models.

Introduction

Osteosarcoma (OS) is the second most common bone cancer after chondrosarcoma, and the most common bone malignancy in adolescents and young adults (1, 2). The 5-year survival rate is <20% for patients with metastatic OS at primary diagnosis, and the median survival after multiple recurrences is only 1 year (3–6). Few new treatment options have been developed for metastatic OS during the past three decades, underscoring the need for novel therapies.

Immunotherapy using monoclonal antibodies (mAbs) specific for overexpressed cancer-related antigens is a promising treatment strategy for micrometastases and circulating tumor cells (7–10). Clinical trials have evaluated the efficacy of mAbs in OS, including trastuzumab targeting the human epidermal growth factor receptor 2 (HER2) (11), glembatumumab targeting glycoprotein nonmetastatic B (12), cixutumumab targeting insulin-like growth factor 1 (13, 14), and pembrolizumab, nivolumab and camrelizumab targeting PD-1 (15–19). Unfortunately, sufficient antitumor response was not demonstrated for OS patients receiving these immune-based therapies, possibly due to low expression of the tumor antigens and internal resistance mechanisms (20, 21). The murine IgG2b TP-3 mAb binds to an 80 kDa sarcoma-associated cell surface membrane antigen (p80) on an alkaline phosphatase isoform (22, 23). TP-3 is directly related to osteoblastic differentiation and has previously shown to bind to the vast majority of OS metastases in patients (23, 24). Moreover, an immunomagnetic isolation procedure using the TP-3 mAb detected single OS cells in bone marrow aspirates from OS patients that was shown to have prognostic information (24, 25). Because of the nonreactive activity of TP-3 on healthy human tissues, it is well suited for targeted therapy (22, 23).

Osteosarcoma is clinically regarded as a radioresistant cancer, and external beam radiotherapy is usually not effective for OS (26–29). Unfortunately, the mechanisms of action related to the radioresistance are not well investigated and remain unresolved (30). Targeted therapies using mAbs labeled with the beta emitting ^{188}Re or ^{177}Lu, and the alpha emitting ^{211}At or ^{213}Bi have been studied for OS *in vitro* and *in vivo* (31–38). However, beta particles have low linear energy transfer (LET, $\sim$ 0.2 keV/μm), making them less effective for treating

radioresistant tumor cells (39). In contrast, alpha particles have a high LET ($\sim$ 100 keV/μm) and short range in tissue (50–100 μm) compared to beta particles (0.5–12 mm), resulting in high cytotoxic potency via DNA double stranded breaks (39). Therefore, alpha particles should be preferred over beta particles to overcome radiation resistance in OS.

The alpha emitting ^{223}Ra (t$_{1/2}$ $\approx$ 11.4 d) is a calcium-mimetic radiopharmaceutical with naturally bone-seeking properties (40, 41). Its accumulation in osteoblastic lesions resulted in improved overall survival and approval for the treatment of castration-resistant prostate cancer patients with symptomatic bone metastases (42). Thus, ^{223}Ra can also be efficient for OS patients due to the osteoblastic phenotype of this cancer (43–46). In 2021, a phase I escalation trial with 50, 75, and 100 kBq/kg of ^{223}Ra was completed in 18 OS patients with progressive, locally recurrent or metastatic disease (3). The radiopharmaceutical was well tolerated and a recommended phase II dose was set to 100 kBq/kg — a twice as high dose as approved for prostate cancer, due to the high radiation tolerance (3). Unfortunately, the majority of patients developed extra-skeletal metastases (3). Since ^{223}Ra cannot be stably chelated to a targeting moiety, it must be combined with other agents that can target extra-skeletal disease in these patient groups (45).

Similar to ^{223}Ra, ^{224}Ra (t$_{1/2}$ $\approx$ 3.6 d) has the same bone-seeking properties, four alpha emissions in the decay chain and a relevant half-life for radiopharmaceutical production and shipment (47). An important difference is that ^{224}Ra decays into ^{212}Pb (t$_{1/2}$ $\approx$ 10.6 h), which, compared to ^{211}Pb (t$_{1/2}$ $\approx$ 36.1 min) in the ^{223}Ra-series, has a convenient half-life for conjugation to targeting molecules (47–49). Lead-212 is itself a beta emitter, but serves as an *in vivo* generator of alpha particles via its decay to ^{212}Bi (t$_{1/2}$ $\approx$ 60.6 min) and ^{212}Po (t$_{1/2}$ $\approx$ 0.3 μs). With the bifunctional 1,4,7,10-tetraaza-1,4,7,10-tetra(2-carbamoylmethyl)cyclododecane (TCMC) chelator for ^{212}Pb, several radioconjugates have been produced and tested in preclinical and clinical studies (49–61). The dual alpha technology utilizes the osteoblastic stroma-seeking properties of ^{224}Ra that can treat primary bone cancer or bone metastases, while extra-skeletal and skeletal metastases can be targeted by a cancer specific moiety labeled with ^{212}Pb (47). In a preclinical prostate cancer study employing this technology, the biodistribution data showed high uptake of ^{224}Ra in the

femur and skull while a ^{212}Pb-conjugate had high prostate tumor uptake (62). The technology also showed promising potential in a breast cancer study, where the ^{224}Ra solution with bone targeting ^{212}Pb-EDTMP [ethylenediamine tetra (methylenephosphonic acid)] prolonged survival and lowered the incidence of bone metastases in mice (63).

Representative *in vitro* models are essential to mimic tumor micrometastases. Three-dimensional (3D) multicellular spheroids have been utilized in preclinical cancer therapy studies since they exhibit physiologically relevant cell–cell and cell–matrix interactions, heterogeneity and structural complexity which better reflect cancer metastases that are found in patients (64–68). The cell–cell interactions allow contribution by the bystander and cross-fire effects to the cytotoxicity of targeted radionuclide therapy to be considered. Spheroids have a necrotic core surrounded by a viable rim of proliferating cells (69), where steep gradients can exist for cellular oxygen levels, proliferation, pH and glucose concentration (70, 71), leading to development of cell subpopulations that may be resistant to treatment, similar to tumor cells *in vivo* (72). Therefore, spheroids are advantageous *in vitro* models because overcoming these factors could not be considered in 2D monolayer models (66, 70).

In this work, the cytotoxic effect of a single alpha solution comprising ^{212}Pb conjugated to the OS cell targeting mAb TP-3 and a dual alpha solution containing ^{224}Ra in equilibrium with ^{212}Pb-TCMC-TP-3 were evaluated using an *in vitro* 3D multicellular spheroid model.

Materials and methods

Cell line

The human OS cell line OHS (established at the Norwegian Radium Hospital) was used in this study (73). The OHS cell line used in the present study was obtained from a repository at the Norwegian Radium Hospital, Oslo University Hospital. The cell line was cultured in RPMI 1640 medium (Sigma-Aldrich Norway AS, Oslo) supplemented with 10% heat inactivated fetal bovine serum (FBS, GE Healthcare Life Sciences, Chicago, IL), 100 units/ml penicillin and 100 μg/ml streptomycin (Sigma-Aldrich) at 37°C with 5% CO_2.

Antibodies

The anti-p80 IgG2b murine mAb TP-3 was produced and purified as described by Bruland et al. (22). TP-3 (PAK-732 batch), was used in all experiments (22, 25). The chimeric anti-CD20 IgG1 mAb rituximab (RTX, MabThera, Roche, Basel) and the humanized anti-HER2 IgG1 mAb trastuzumab (TRA, Herceptin, Roche) were used as antigen negative controls.

Flow cytometry

The expression of p80 on OHS cells was verified by flow cytometry using TP-3. The primary mAbs (TP-3 or RTX) were added to 5×10^5 OHS cells in 100 μl flow buffer [Dulbecco's PBS with 0.5% bovine serum albumin (BSA) and 0.1% NaN_3] at a concentration of 10 μg/ml and incubated at 4°C with gentle shaking for 60 min, followed by three washes with 2 ml flow buffer. FITC-conjugated anti-mouse IgG F(ab')2 fragment (Thermo Fisher Scientific, Waltham, MA) was used as a secondary Ab and added at a concentration of 10 μg/ml, incubated at 4°C with gentle shaking for 30 min in the dark and washed as in the previous step. All wash steps were performed by centrifugation at $260 \times g$ for 5 min. Washed cell pellets were resuspended in 200 μl flow buffer and analyzed by a Cytoflex S flow cytometer (Beckman Coulter, Inc., Brea, CA) using the CytExpert 2.0 software (Beckman Coulter, Inc.) for data acquisition. The FlowJo software (FlowJo, LLC, Ashland, OR) was used for data analysis.

Preparation of radionuclides and activity measurements

Radium-224 was extracted from a generator column containing DIPEX® actinidine resin (Eichrom Technologies, Lisle, IL) with immobilized ^{228}Th (Eckert & Ziegler, Braunschweig) by elution with 1 M HCl. The details of the ^{224}Ra generator setup have previously been described by Westrøm et al. and Stenberg et al. (62, 74). Lead-212 was produced and extracted from a ^{228}Th generator, via emanation of ^{220}Rn in a simplified single-chamber generator system, described by Li et al. (75). Lead-212 was extracted from the flask using 0.1 M HCl, with a ^{228}Th breakthrough ≤0.005%. The collector flask was replaced 2–3 days prior to the experiments to prevent accumulation of ^{208}Pb. A Capintec CRC-25R radioisotope dose calibrator (Capintec Inc., Ramsey, NJ) was used to quantify the ^{224}Ra and ^{212}Pb activities (76).

A Hidex automatic gamma counter (Hidex Oy, Turku) or Cobra gamma counter (Packard Instrument Company, Downer Grove, IL) with the 50–120 keV counting window was used to determine ^{212}Pb activities. The counting window mainly measures ^{212}Pb activity (34.9% relative to the ^{224}Ra mother nuclide) with only small contribution from other radionuclides (1.2% relative to ^{224}Ra) in the ^{224}Ra series (47, 62, 74, 77). All samples were measured at least 2 h after ^{212}Pb extraction to ensure transient equilibrium with daughters. The activity of ^{224}Ra was determined by measurements performed 4–5 days after the experiment, when ^{212}Pb had decayed and equilibrium between ^{224}Ra and the newly formed ^{212}Pb was reached.

Radiolabeling of antibodies

The mAbs were conjugated to a TCMC chelator (Macrocyclics Inc., Dallas, TX), to allow radiolabeling with ^{212}Pb. The original buffer of the mAbs was first exchanged with carbonate buffer (0.1 M NaHCO$_3$ and 5 mM Na$_2$CO$_3$ in metal free water) by washing the mAb solution through a centrifugal concentrator (30 kDa, Amicon Ultra-15 Centrifugal Filter Unit, Millipore, Sigma-Aldrich) three times at $1620 \times g$ for 15–25 min. A TCMC solution in 5 mM HCl was added to the Abs in a 5:1 molar ratio, and the mixture were allowed to react for 2 h with gentle shaking (250 min^{-1}) at room temperature. Then, unconjugated TCMC was removed from TCMC-mAb conjugates by exchanging the carbonate buffer to 0.9% NaCl by washing the mAb solution through the centrifugal concentrator as described above. The concentration of the mAbs was quantified by Nanodrop (Nanodrop 1000 Spectrophotometer, V3.8, Thermo Fisher Scientific), using the standard absorbance value of IgG at 280 nm and 10 mm path length.

The mAbs were labeled with ^{212}Pb using ^{224}Ra or ^{212}Pb solutions (pH adjusted to 5–6 by 0.5 M C$_2$H$_7$NO$_2$ or C$_2$H$_3$NaO$_2$) in equilibrium with daughters. TCMC-TP-3, TCMC-RTX, or TCMC-TRA was added to a final concentration of 0.1–1 mg/ml. The solutions were mixed on a Thermomixer (Eppendorf, Hamburg) for 45 min at 37°C and 450–750 rpm. Radiochemical purity of the samples was determined by instant thin layer chromatography (Tec-control, Biodex, Medical Systems, Shirley, NY), and only products with purities ≥95% were used in the experiments. The final solution consisting of ^{212}Pb-TCMC-mAb is referred to as the "single alpha solution" while ^{212}Pb-labeled mAbs in the presence of ^{224}Ra is called the "dual alpha solution."

Saturation binding studies

OHS cells were detached from a cell culture flask using TrypLE Express (Sigma-Aldrich). Saturation binding studies of ^{212}Pb-TCMC-TP-3 to OHS cells were performed by collecting 10^6 of the cells and incubating them as cell suspension in 0.2 ml of PBS including 0.5% BSA (Sigma-Aldrich) with 6 different concentrations (0.03–10 µg/ml) of the radioimmunoconjugate (in duplicates) for 1 h at 37°C and 150 min^{-1}. Non-specific binding was measured by pre-incubating cells with unlabeled TP-3 (5–20 µg/ml) for 15 min before addition of ^{212}Pb-TCMC-TP-3. Activities were measured in a gamma counter before (added activity) and after incubated cells were washed 3 times with PBS containing 0.5% BSA (cell bound activity). Specific cell bound activity was estimated as percentage of added activity minus non-specific binding (activity on blocked cells). The number of specifically bound ligands per cell was plotted against ligand concentration and the equilibrium dissociation constant (K$_D$) and the number of specific binding sites (Bmax), were determined by nonlinear regression (Sigmaplot version 14.5, Systat Software, Inc., San Jose, CA, USA).

Spheroid formation and treatment

Multicellular tumor spheroids were generated using the liquid-overlay technique (78, 79). Spheroids were formed by seeding 500 OHS cells in 100 µl of culture medium per well in a 96-well flat-bottom plate coated with 50 µl of 1.5% agarose (weight/volume, Sigma-Aldrich) solution in PBS (Sigma Aldrich). The plates were centrifuged at $470–1000 \times g$ for 15 min, and maintained at 37°C with 5% CO$_2$.

For the single alpha solution studies, spheroids were treated 4–5 days after formation (day 0) with 0.3–100 kBq/ml of ^{212}Pb-TCMC-TP-3 (specific activities of 7.3–15.4 MBq/mg) or ^{212}Pb-TCMC-RTX (specific activities of 7.5–9.9 MBq/mg). For the dual alpha solution studies, 0.3–10 kBq/ml of ^{224}Ra/^{212}Pb, ^{224}Ra/^{212}Pb-TCMC-TP-3 (specific activities of 2.3–9 MBq/mg), or ^{224}Ra/^{212}Pb-TCMC-RTX/TRA (specific activities of 3.7–9 MBq/mg) were added 3 or 14 days after spheroids were formed. One experiment with TP-3 alone (0.25 µg per spheroid 2.1 µg/ml) was performed in OHS spheroids to investigate the cytotoxicity of the mAb itself. The spheroids were incubated with the mAb alone or with radioconjugates at 37°C for 1, 4, or 24 h before they were carefully washed 6 times with medium and further incubated for 3 weeks. Replacement of culture medium was performed 2–3 times per week. The spheroid diameter (d) was measured weekly using an inverted Axiovert 200M microscope (Carl Zeiss AG, Jena, Germany). Volumes of each spheroid were calculated using the formula $V = \frac{4}{3}\pi r^3$, where r = d/2. The spheroid volumes were normalized by dividing the volumes at different activities by the volume at 0 kBq/ml at each time point (activity vs. normalized volume), and by dividing the volumes of the treated spheroids at each week by the volume of spheroids at day 0 for each activity concentration (time vs. normalized volume).

A CellTiter-Glo®3D cell viability assay (Promega Corporation, Madison, WI, USA), was performed 48 h, 72 h and 12 days after spheroids were administered with ^{224}Ra/^{212}Pb, ^{224}Ra/^{212}Pb-TCMC-TP-3 and ^{224}Ra/^{212}Pb-TCMC-TRA for 24 h according to the manufacture's protocol.

Live and dead cells in the spheroids were determined by a fluorescence-based staining assay using fluorescein diacetate (FDA, 5 mg/ml, Sigma-Aldrich) and propidium iodide (PI, 2 mg/ml, Sigma-Aldrich), respectively. Fluorescent images of spheroids were taken by an inverted Axiovert 200M microscope (Carl Zeiss AG) and analyzed with the AxioVision Rel. 4.8 software (Carl Zeiss AG). The experiment was performed with 3–12 spheroids per treatment condition. The relative viability was calculated by dividing the viability of the treated spheroid by the viability of the control spheroid (0 kBq/ml) at different activity concentrations.

Complete growth inhibition of a spheroid was considered when no live cells were detected in the spheroid, or when the spheroid diameter was reduced or remained unchanged, or when the spheroid was disintegrated/fell apart.

Statistical analyses

SigmaPlot 14.5 (Systat Software) was used for the statistical analyses. Nonlinear regression with one-site saturation ligand binding was used to estimate the number of specific binding sites (B_{max}) and the equilibrium dissociation constant (K_D) for ^{212}Pb-TCMC-TP-3 on the OHS cells:

$$B = \frac{Bmax \times [Ab]}{K_D + [Ab]}$$

where B is the number of antigens per cell and [Ab] is the Ab concentration. Exponential decay fitting was used to plot the correlation between the radioactivity and spheroid volume.

The spheroid volumes and viabilities were analyzed for significance using a one-way ANOVA with multiple comparisons and a pairwise t-test, respectively, using SigmaPlot 14.5 (Systat Software). A p-value of < 0.05 was considered statistically significant.

Results

Binding of TP-3

A high expression of p80 was confirmed by a well-defined histogram shape of TP-3, which demonstrated binding to 99.7% of the OHS cells with no overlap and clear separation from the histograms representing the control samples (**Figure 1A**). Negligible non-specific binding was detected ($< 0.06\%$) as the histogram of RTX was identical as the unstained cells and the secondary Ab control.

The OHS cells showed an average of $2.7 \pm 0.3 \times 10^5$ binding sites per cell (B_{max}). The ^{212}Pb-TCMC-TP-3 demonstrated increased binding to OHS cells at 0.03–1 µg/ml after 1 h with a K_D of 0.49 ± 0.05 µg/ml (**Figure 1B**). Similar levels of ^{212}Pb-TCMC-TP-3 were bound to the OHS cells at 4 h (**Supplementary Figure 1**). From 1 to 10 µg/ml, the percentage of specific bound ^{212}Pb-TCMC-TP-3 was reduced due to saturated binding sites (**Figure 1C**). Of total added radioimmunoconjugate, 5.7–12.2% was internalized to the cells after 1 h (**Supplementary Figure 1**).

Cytotoxicity of the ^{212}Pb-TCMC-TP-3 single alpha solution

The spheroids had a diameter of 253 ± 98 µm and a volume of $8.5 \pm 0.5 \times 10^6$ µm^3 at day 0 (treatment day). The majority
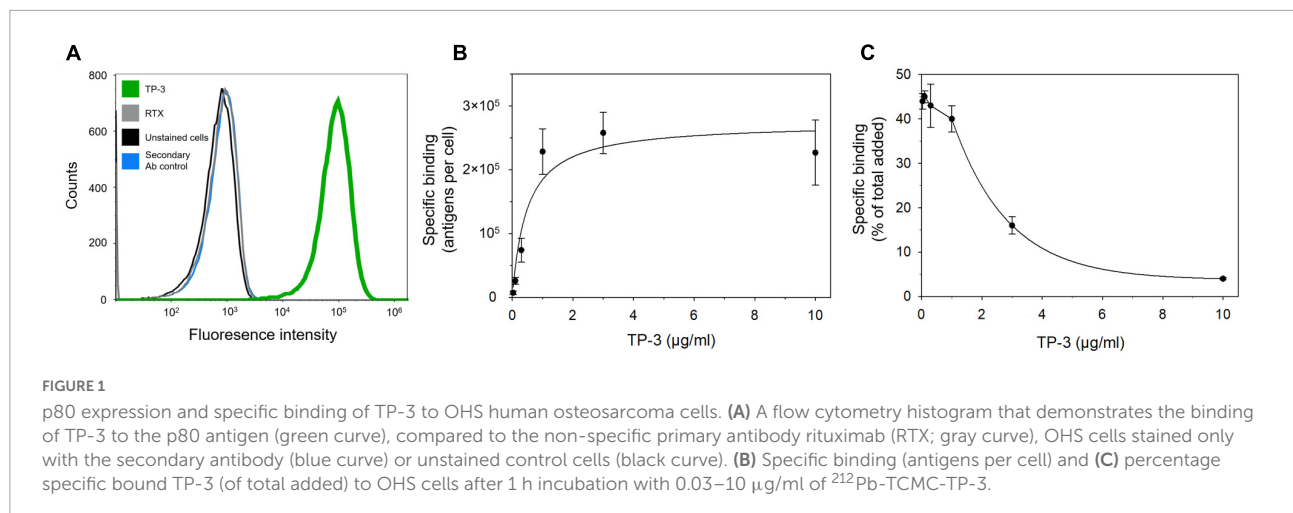
of OHS cells in these spheroids were viable at this time point (**Supplementary Figure 6**). The volume of spheroids decreased with increasing ^{212}Pb-TCMC-TP-3 activity (**Figure 2A** and **Supplementary Figure 2**). At 3 weeks, 1 and 4 h incubation with 2.7–9 kBq/ml of ^{212}Pb-TCMC-TP-3 significantly inhibited the spheroid growth and reduced the number of live cells compared to the control ($p < 0.005$, **Figures 2B,C**, **Supplementary Figures 3, 4**, and **Supplementary Table 3**). The doubling time was 7-fold longer for the spheroids treated with 2.7 kBq/ml of ^{212}Pb-TCMC-TP-3 for 4 h compared to the control, while 6.3-fold longer than for the spheroids treated with 75 kBq/ml of ^{212}Pb-TCMC-RTX (**Supplementary Table 1**). After 3 weeks, no live cells or spheroid growth were detected in the spheroids treated with ≥ 2.7 kBq/ml of ^{212}Pb-TCMC-TP-3 for 4 and 24 h (**Figure 2C** and **Supplementary Figures 4, 5**). The non-specific ^{212}Pb-TCMC-RTX was only able to completely inhibit spheroid growth after 3 weeks when treated with the high activity dose of 72.8 kBq/ml for 24 h (**Supplementary Figure 5**).

Cytotoxicity of the ^{224}Ra/^{212}Pb-TCMC-TP-3 dual alpha solution

The cytotoxicity of the dual alpha solutions was investigated in small (diameter of 222 ± 14.0 µm and volume of $5.8 \pm 1.0 \times 10^6$ µm^3 at day 0) and large (diameter of 474 ± 2 µm and volume of $60 \pm 5.0 \times 10^6$ µm^3 at day 0) spheroids. The majority of OHS cells in the small spheroids were viable, while the large spheroids developed central necrosis with a 20–30 µm rim of viable cells (**Supplementary Figure 6**). All spheroid volumes were reduced at increasing activities, and the growth of spheroids treated for 4 or 24 h with ≥ 5 kBq/ml of ^{224}Ra/^{212}Pb-TCMC-TP-3 was completely inhibited (**Figure 3** and **Supplementary Figure 7**).

Over time, the volume of spheroids treated with 1 kBq/ml of ^{224}Ra/^{212}Pb or ^{224}Ra/^{212}Pb-TCMC-RTX for 4 h increased, whereas this activity concentration of ^{224}Ra/^{212}Pb-TCMC-TP3 inhibited spheroid growth (**Supplementary Figure 7**). The doubling time of spheroids treated with 10 kBq/ml of ^{224}Ra/^{212}Pb-TCMC-TP-3 for 1 h was 101 days, while it was 15 and 22 days for spheroids treated with ^{224}Ra/^{212}Pb and ^{224}Ra/^{212}Pb-TCMC-RTX, respectively (**Supplementary Table 2**).

A viability assay was performed for spheroids treated with the dual alpha solutions for 24 h. At 72 h, a significant reduction in viability was seen in the spheroids treated with 5 kBq/ml of ^{224}Ra/^{212}Pb-TCMC-TP-3 versus ^{224}Ra/^{212}Pb or ^{224}Ra/^{212}Pb-TCMC-TRA ($p < 0.05$, **Supplementary Table 4**). Twelve days after treatment, the relative viabilities of the spheroids treated with 1 kBq/ml of the ^{224}Ra/^{212}Pb-TCMC-TP-3, ^{224}Ra/^{212}Pb and ^{224}Ra/^{212}Pb-TCMC-TRA dual alpha solutions were 11.6 ± 2.7, 56.2 ± 6.6 and 47.2 ± 6, respectively (**Figure 4A**).

FIGURE 1
p80 expression and specific binding of TP-3 to OHS human osteosarcoma cells. **(A)** A flow cytometry histogram that demonstrates the binding of TP-3 to the p80 antigen (green curve), compared to the non-specific primary antibody rituximab (RTX; gray curve), OHS cells stained only with the secondary antibody (blue curve) or unstained control cells (black curve). **(B)** Specific binding (antigens per cell) and **(C)** percentage specific bound TP-3 (of total added) to OHS cells after 1 h incubation with 0.03–10 μg/ml of ^{212}Pb-TCMC-TP-3.

Complete disintegration was observed for all spheroids incubated for 24 h with 10 kBq/ml of any dual alpha solution. However, only spheroids treated with the ^{224}Ra/^{212}Pb-TCMC-TP-3 dual alpha solution were disintegrated 12 days after incubation with 5 kBq/ml (**Figure 4B**), while the relative viability of spheroids treated with ^{224}Ra/^{212}Pb and ^{224}Ra/^{212}Pb-TCMC-TRA were 8.0 ± 3.4 and 7.4 ± 2.4 at this time point, respectively.
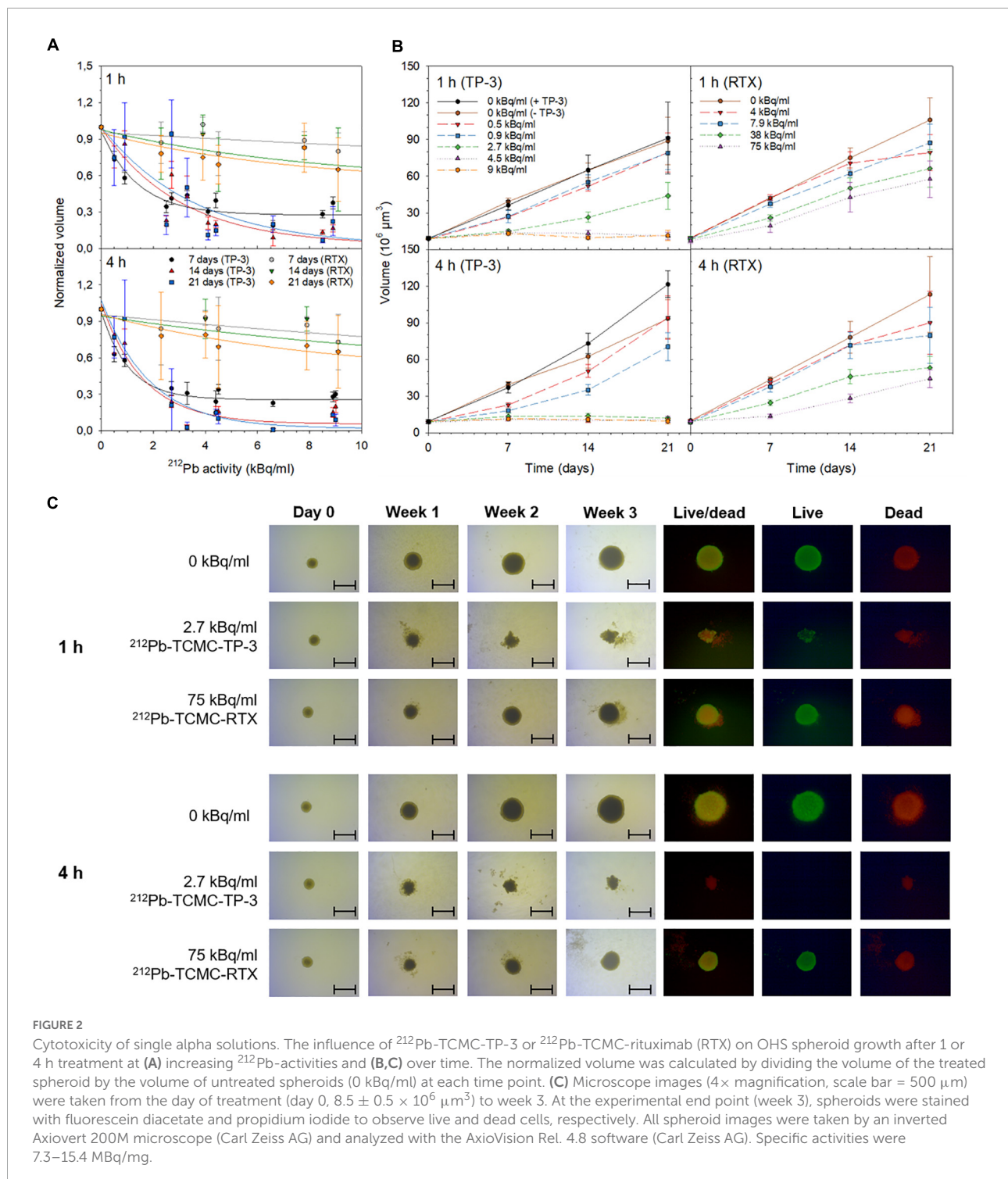
Discussion

The treatment options for advanced OS after standard regimen are limited due to chemotherapeutic resistance (80–82). Micrometastases are found in the majority of patients with advanced and/or recurrent OS (25, 83). Patients with micrometastases in the bone marrow or peripheral blood, also from other forms of cancer than OS, have shown statistically poorer survival compared to patients without micrometastases (25, 82, 84–88). The size of spheroids used in the present study was chosen based on a previous study by Däster et al. (89). In agreement with the study, the small spheroids herein consisted almost entirely of viable cells, while the large spheroids had a necrotic core surrounded by a rim of viable cells (**Supplementary Figure 6**). The single and dual alpha solutions containing TP-3 were able to disintegrate spheroids with diameters ranging from 210 to 480 μm, which is similar to the diameter of micrometastatic clusters found in patients (250–750 μm) (65, 90, 91). As already mentioned, TP-3 has previously shown the ability to detect single micrometastatic cells in bone marrow aspirates from OS patients, in which a strong correlation was detected between the TP-3 bound OS cells and poor therapeutic response following relapse (24, 25). In the present study, the TP-3 mAb itself did not initiate any cytotoxicity on OHS multicellular spheroids, which is in agreement with a previous study (33).

In contrast, the cytotoxic effect was significantly improved when spheroids were treated with ≥ 2.7 kBq/ml of the ^{212}Pb-TCMC-TP-3 radioimmunoconjugate ($p < 0.005$, **Figure 2** and **Supplementary Table 3**). The therapeutic efficacy of ^{211}At-TP-3 was extensively explored three decades ago and showed promising potential for OS *in vitro* and *in vivo*, similar to a more recent study evaluating a ^{213}Bi radioimmunoconjugate (33–35, 38, 92). Unfortunately, challenges related to the production of ^{211}At and the very short half-life of ^{213}Bi limits the applicability of these radionuclides in targeted therapy. TP-3 immunotoxins have previously showed to be effective in clonogenic OS cells *in vitro*, and in a subcutaneous as well as in a soft-tissue sarcoma model *in vivo* (93–95). SCID mice xenografted with OHS cells were treated with 1.0 mg/kg of a TP-3 immunotoxin and 67 ± 19% of the mice were tumor-free at 150 days, compared to the control mice which had a median survival of 19 days (94). Despite these encouraging data, immunogenicity and nonspecific toxicity is known to limit the clinical success of immunotoxins (96). Nevertheless, TP-3 seems highly promising for targeted therapies because of the high expression levels of p80 on the OS cell surface and the limited normal-tissue distribution (22, 23).

An important advantage with the 3D spheroid model is the possibility to observe the treatment response over an extended period, and thereby observe the repopulation potential of surviving cells. After 1 week, the volume of spheroids treated with 2.7 kBq/ml of ^{212}Pb-TCMC-TP-3 for 1 h looked similar as spheroids treated with 4.5 and 9 kBq/ml (**Figure 2B**). Yet, regrowth of the spheroids was seen from week 2. After 4 h incubation with 2.7 kBq/ml of the ^{212}Pb-TCMC-TP-3 single alpha solution, spheroids were disintegrated and no viable cells were observed at week 3 (**Figure 2**). This cytotoxic effect is similar to a study investigating comparable activities of ^{212}Pb in 3D prostate cancer spheroids (52). A study by

FIGURE 2

Cytotoxicity of single alpha solutions. The influence of ^{212}Pb-TCMC-TP-3 or ^{212}Pb-TCMC-rituximab (RTX) on OHS spheroid growth after 1 or 4 h treatment at **(A)** increasing ^{212}Pb-activities and **(B,C)** over time. The normalized volume was calculated by dividing the volume of the treated spheroid by the volume of untreated spheroids (0 kBq/ml) at each time point. **(C)** Microscope images (4× magnification, scale bar = 500 μm) were taken from the day of treatment (day 0, $8.5 \pm 0.5 \times 10^6$ μm^3) to week 3. At the experimental end point (week 3), spheroids were stained with fluorescein diacetate and propidium iodide to observe live and dead cells, respectively. All spheroid images were taken by an inverted Axiovert 200M microscope (Carl Zeiss AG) and analyzed with the AxioVision Rel. 4.8 software (Carl Zeiss AG). Specific activities were 7.3−15.4 MBq/mg.

Ballangrud et al. investigated the therapeutic effect of a ^{213}Bi labeled mAb in multicellular prostate cancer spheroids with a diameter of 200 μm, and showed that the penetration time of the radioimmunoconjugate was around 3 h (97). This supports the results observed herein, where a substantial increased cytotoxic effect was seen in spheroids (diameter of

253 ± 98 μm) treated with 2.7 kBq/ml of ^{212}Pb-TCMC-TP-3 when the treatment duration increased from 1 to 4 h (Figure 2). These results are also in agreement with Hjelstuen et al. who demonstrated that 6 h was required for the ^{125}I labeled mAb to reach the inner center of an OHS spheroid with a diameter of 400−450 μm (98). Nevertheless, because of the
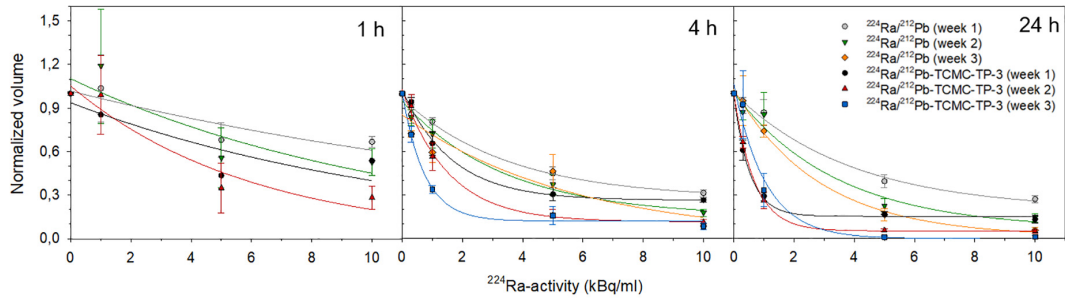
FIGURE 3

Cytotoxicity of dual alpha solutions. The influence of 1, 4, or 24 h incubation of ^{224}Ra/^{212}Pb and ^{224}Ra/^{212}Pb-TCMC-TP-3 on OHS spheroid growth at increasing ^{224}Ra/^{212}Pb-activities. The normalized volume was calculated by dividing the volume of the treated spheroid by the volume of untreated spheroids at each week. Spheroids were 5.8−60 × 10^6 μm^3 at day 0. Specific activities were 2.3−9 MBq/mg.
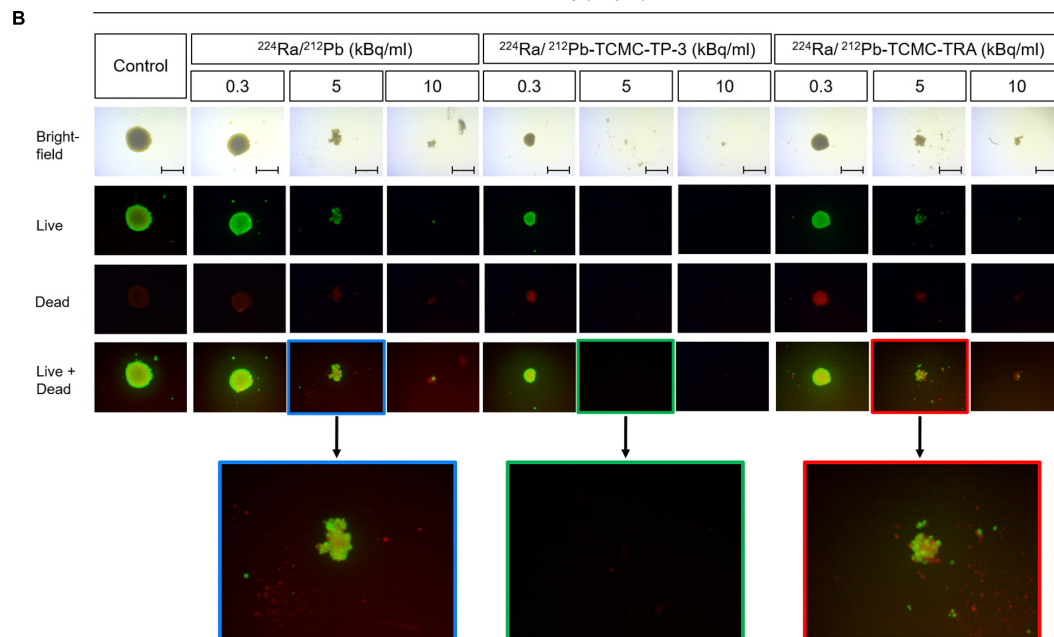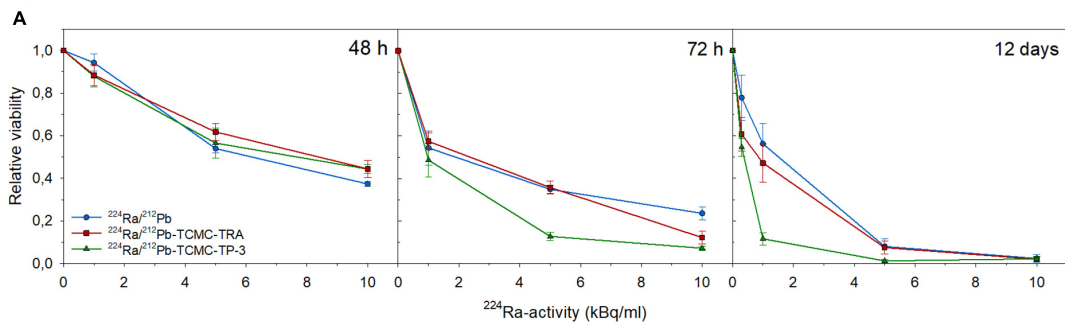

FIGURE 4

Viability of OHS spheroids treated with dual alpha solutions. **(A)** Viability of spheroids 48 h, 72 h, and 12 days after 24 h incubation with 1−10 kBq/ml of ^{224}Ra/^{212}Pb, ^{224}Ra/^{212}Pb-TCMC-TP-3 (specific activity of 2.3 MBq/mg) or ^{224}Ra/^{212}Pb-TCMC-trastuzumab (TRA, specific activity of 3.7 MBq/mg). The relative viability was calculated by dividing the viability of the treated spheroids by the viability of untreated spheroids (0 kBq/ml) at each activity concentration. **(B)** At day 12, spheroids were stained with fluorescein diacetate and propidium iodide to observe live and dead cells, respectively, before spheroids were imaged (4× magnification) using an inverted Axiovert 200M microscope (Carl Zeiss AG, Jena, Germany), scale bar = 500 μm. All spheroids were analyzed with the AxioVision Rel. 4.8 software (Carl Zeiss AG). Spheroids were 60 ± 5.0 × 10^6 μm^3 at day 0.

short half-life of ^{213}Bi ($t_{1/2} \approx 46$ min), 76% of the decay in Ballangrud's study had already occurred by the time that the radioimmunoconjugate reached the inner core of the spheroid (97). This highlights the benefit of labeling a targeting molecule with ^{212}Pb, as it has a long enough half-life for the majority of the deposited energy from the total decay to be emitted within the spheroid. However, it is important to mention that the OS tumor microenvironment is highly complex and the penetration time will also depend on other factors such as density and vascularity enabling diffusion of the targeting complex (70).

The growth inhibition of spheroids observed 3 weeks after 4 h treatment with 2.7–4.5 kBq/ml of the ^{212}Pb-TCMC-TP-3 single alpha solution (Figure 2 and Supplementary Figure 4) and 5 kBq/ml of the ^{224}Ra/^{212}Pb-TCMC-TP-3 dual alpha solution (Figure 3 and Supplementary Table 2) corresponds to 13.5–22.5 MBq of ^{212}Pb and 25 MBq of ^{224}Ra per patient ($\sim$ 5 L blood). Subbiah et al. recommended an activity of 100 kBq/kg of ^{223}RaCl$_2$ for the phase II study in OS patients (3). Assuming similar clinical dosing of ^{224}Ra as for ^{223}Ra (taken the different half-lives into account), this would translate into a clinically relevant dosage of 315 kBq/kg of ^{224}Ra. In equilibrium with daughters, the ^{212}Pb-immunoconjugate in the dual alpha solution would then be given in a dosage of approximately 24 MBq per patient ($\sim$ 70 kg). This falls within the activity range of the ^{212}Pb-TCMC-TRA radioimmunoconjugate (13–47 MBq) that was evaluated as safe for patients with HER2 overexpressing intraperitoneal cancer (55). This suggests that ^{224}Ra/^{212}Pb-TCMC-TP-3 induces cytotoxic effects at clinically relevant activity doses, although activity conversions from mouse to human also may be based on body surface area and not only on radioactivity per gram of bodyweight or blood (99).

Limitations of this study include the use of non-osteoblastic OHS spheroids, leading to an insignificant improvement in cytotoxicity from the naturally bone-seeking ^{224}Ra itself. Therefore, the dual alpha solution with TP-3 required similar activities to disintegrate spheroids as the single alpha solution, meaning that the antitumor effect of the multicellular spheroids was likely linked to the delivery of the radiation emitted from the specifically bound ^{212}Pb-TCMC-TP-3. Preincubation of OS cells in a calcifying medium can force the cells into an osteoblastic-like state, which will enhance the similarity of a true OS microenvironment such as observed in patients, and thereby potentially initiate an effect of ^{224}Ra (100). This should be evaluated in future studies using multicellular spheroid models of OS. Furthermore, following the protocol of Jacques et al., establishing a murine model with bone sarcoma would be the next step to fully explore the potential of the dual alpha *in vivo* (101). Nonetheless, previous dual alpha studies have verified that ^{224}Ra accumulates in bone (62, 63). In fact, in a preclinical breast cancer study, a ^{224}RaCl$_2$ solution

with the ^{212}Pb-daughter chelated to the bone-seeking EDTMP demonstrated similar therapeutic effect as a comparable *in vivo* study with ^{223}RaCl$_2$, but with significantly fewer radium atoms (47, 63, 102). A ^{224}Ra solution without a chelating agent for the lead-daughter, such as for the approved ^{223}RaCl$_2$, will also have bone-seeking properties, but since ^{212}Pb have a half-life that allows trans-organ redistribution if let free in physiological liquids like blood, saliva or lymphatic liquid, the toxicity impact from ^{212}Pb is important to consider and will be minimized by the conjugation to TP-3 or EDTMP. An experimental limitation in this study includes adding activities from the single and dual alpha solutions to spheroids of different size. Ideally, the single and dual alpha experiments should be performed simultaneously with similar spheroid size at day 0. This should be considered in future studies.

Conclusion

This study demonstrated high cytotoxicity at clinically relevant activities of the single and dual alpha solutions in spheroids mimicking micrometastatic OS disease. These results warrant further exploration in preclinical models to evaluate the therapeutic efficacy and cytotoxicity of the ^{224}Ra/^{212}Pb-TCMC-TP-3 dual alpha solution in an osteoblastic OS environment.

Data availability statement

The original contributions presented in this study are included in the article/Supplementary material, further inquiries can be directed to the corresponding author.

Author contributions

AJKT, AJ, ØSB, and RHL: conceptualization. AJKT, AJ, VYS, ØSB, and RHL: designing the work. AJKT and AJ: *in vitro* experiments. AJKT, AJ, and VYS: analyzing the data. AJ, AJKT, VYS, ØSB, M-ER, and RHL: interpretation of results and drafting the manuscript and revising it critically for important intellectual content. All authors read and agreed to the published version of the manuscript.

Funding

Oslo, Norway) and the South-Eastern Norway Regional Health Authority (project number: 2020028, Oslo, Norway).

Conflict of interest

Authors ØSB and RHL hold ownership interest in ArtBio AS.

The remaining authors declare that the research was conducted in the absence of any commercial or financial relationships that could be construed as a potential conflict of interest.

Publisher's note

All claims expressed in this article are solely those of the authors and do not necessarily represent those of their affiliated organizations, or those of the publisher, the editors and the reviewers. Any product that may be evaluated in this article, or claim that may be made by its manufacturer, is not guaranteed or endorsed by the publisher.

Supplementary material

The Supplementary Material for this article can be found online at: https://www.frontiersin.org/articles/10.3389/fmed.2022.1058863/full#supplementary-material

References

1. Mirabello L, Troisi RJ, Savage SA. Osteosarcoma incidence and survival rates from 1973 to 2004: data from the surveillance, epidemiology, and end results program. *Cancer*. (2009) 115:1531–43.

2. Cole S, Gianferante DM, Zhu B, Mirabello L. Osteosarcoma: a surveillance, epidemiology, and end results program-based analysis from 1975 to 2017. *Cancer*. (2022) 128:2107–18. doi: 10.1002/cncr.34163

3. Subbiah V, Anderson PM, Kairemo K, Hess K, Huh WW, Ravi V, et al. Alpha particle radium 223 dichloride in high-risk osteosarcoma: a phase i dose escalation trial. *Clin Cancer Res*. (2019) 25:3802–10.

4. Berner K, Johannesen TB, Berner A, Haugland HK, Bjerkehagen B, Bøhler PJ, et al. Time-trends on incidence and survival in a nationwide and unselected cohort of patients with skeletal osteosarcoma. *Acta Oncol*. (2015) 54:25–33. doi: 10.3109/0284186X.2014.923934

5. Berner K, Hall KS, Monge OR, Weedon-Fekjær H, Zaikova O, Bruland ØS. Prognostic factors and treatment results of high-grade osteosarcoma in Norway: a scope beyond the "classical" patient. *Sarcoma*. (2015) 2015:516843. doi: 10.1155/2015/516843

6. Anderson P, Aguilera D, Pearson M, Woo S. Outpatient chemotherapy plus radiotherapy in sarcomas: improving cancer control with radiosensitizing agents. *Cancer Control*. (2008) 15:38–46. doi: 10.1177/107327480801500105

7. Zahavi D, Weiner L. Monoclonal antibodies in cancer therapy. *Antibodies*. (2020) 9:34.

8. Jin S, Sun Y, Liang X, Gu X, Ning J, Xu Y, et al. Emerging new therapeutic antibody derivatives for cancer treatment. *Signal Transduct Target Ther*. (2022) 7:39.

9. Oldham RK, Dillman RO. Monoclonal antibodies in cancer therapy: 25 years of progress. *J Clin Oncol*. (2008) 26:1774–7.

10. Pantel K, Alix-Panabières C. Circulating tumour cells in cancer patients: challenges and perspectives. *Trends Mol Med*. (2010) 16:398–406.

11. Ebb D, Meyers P, Grier H, Bernstein M, Gorlick R, Lipshultz SE, et al. Phase II trial of trastuzumab in combination with cytotoxic chemotherapy for treatment of metastatic osteosarcoma with human epidermal growth factor receptor 2 overexpression: a report from the children's oncology group. *J Clin Oncol*. (2012) 30:2545–51. doi: 10.1200/JCO.2011.37.4546

12. Kopp LM, Malempati S, Krailo M, Gao Y, Buxton A, Weigel BJ, et al. Phase II trial of the glycoprotein non-metastatic B-targeted antibody-drug conjugate, glembatumumab vedotin (CDX-011), in recurrent osteosarcoma AOST1521: a report from the Children's oncology group. *Eur J Cancer*. (2019) 121:177–83. doi: 10.1016/j.ejca.2019.08.015

13. Weigel B, Malempati S, Reid JM, Voss SD, Cho SY, Chen HX, et al. Phase 2 trial of cixutumumab in children, adolescents, and young adults with refractory solid tumors: a report from the Children's oncology group. *Pediatr Blood Cancer*. (2014) 61:452–6. doi: 10.1002/pbc.24605

14. Malempati S, Weigel B, Ingle AM, Ahern CH, Carroll JM, Roberts CT, et al. Phase I/II trial and pharmacokinetic study of cixutumumab in pediatric patients with refractory solid tumors and Ewing sarcoma: a report from the Children's oncology group. *J Clin Oncol*. (2012) 30:256–62. doi: 10.1200/JCO.2011.37.4355

15. Le Cesne A, Marec-Berard P, Blay JY, Gaspar N, Bertucci F, Penel N, et al. Programmed cell death 1 (PD-1) targeting in patients with advanced osteosarcomas: results from the PEMBROSARC study. *Eur J Cancer*. (2019) 119:151–7. doi: 10.1016/j.ejca.2019.07.018

16. Tawbi HA, Burgess M, Bolejack V, Van Tine BA, Schuetze SM, Hu J, et al. Pembrolizumab in advanced soft-tissue sarcoma and bone sarcoma (SARC028): a multicentre, two-cohort, single-arm, open-label, phase 2 trial. *Lancet Oncol*. (2017) 18:1493–501. doi: 10.1016/S1470-2045(17)30624-1

17. Boye K, Longhi A, Guren T, Lorenz S, Næss S, Pierini M, et al. Pembrolizumab in advanced osteosarcoma: results of a single-arm, open-label, phase 2 trial. *Cancer Immunol Immunother*. (2021) 70:2617–24. doi: 10.1007/s00262-021-02876-w

18. D'Angelo SP, Mahoney MR, Van Tine BA, Atkins J, Milhem MM, Jahagirdar BN, et al. Nivolumab with or without ipilimumab treatment for metastatic sarcoma (Alliance A091401): two open-label, non-comparative, randomised, phase 2 trials. *Lancet Oncol*. (2018) 19:416–26.

19. Xie L, Xu J, Sun X, Guo W, Gu J, Liu K, et al. Apatinib plus camrelizumab (anti-PD1 therapy, SHR-1210) for advanced osteosarcoma (APFAO) progressing after chemotherapy: a single-arm, open-label, phase 2 trial. *J Immunother Cancer*. (2020) 8:e000798.

20. Wedekind MF, Wagner LM, Cripe TP. Immunotherapy for osteosarcoma: where do we go from here? *Pediatr Blood Cancer*. (2018) 65:e27227. doi: 10.1002/pbc.27227

21. Prudowsky ZD, Yustein JT. Recent insights into therapy resistance in osteosarcoma. *Cancers*. (2020) 13:83.

22. Bruland O, Fodstad O, Funderud S, Pihl A. New monoclonal antibodies specific for human sarcomas. *Int J Cancer*. (1986) 38:27–31.

23. Bruland OS, Fodstad O, Stenwig AE, Pihl A. Expression and characteristics of a novel human osteosarcoma-associated cell surface antigen. *Cancer Res.* (1988) 48:5302–9.

24. Bruland OS, Høifødt H, Saeter G, Smeland S, Fodstad O. Hematogenous micrometastases in osteosarcoma patients. *Clin Cancer Res.* (2005) 11:4666–73.

25. Bruland ØS, Høifødt H, Hall KS, Smeland S, Fodstad Ø. Bone marrow micrometastases studied by an immunomagnetic isolation procedure in extremity localized non-metastatic osteosarcoma patients. *Cancer Treat Res.* (2009) 152:509–15. doi: 10.1007/978-1-4419-0284-9_30

26. Biazzo A, De Paolis M. Multidisciplinary approach to osteosarcoma. *Acta Orthop Belg.* (2016) 82:690–8.

27. Weichselbaum R, Little JB, Nove J. Response of human osteosarcoma in vitro to irradiation: evidence for unusual cellular repair activity. *Int J Radiat Biol Relat Stud Phys Chem Med.* (1977) 31:295–9. doi: 10.1080/09553007714550351

28. Spałek MJ, Poleszczuk J, Czarnecka AM, Dudzisz-Śledź M, Napieralska A, Matysiakiewicz J, et al. Radiotherapy in the management of pediatric and adult osteosarcomas: a multi-institutional cohort analysis. *Cells.* (2021) 10:366. doi: 10.3390/cells10020366

29. Schwarz R, Bruland O, Cassoni A, Schomberg P, Bielack S. The role of radiotherapy in osteosarcoma. *Cancer Treat Res.* (2009) 152:147–64. doi: 10.1007/978-1-4419-0284-9_7

30. Koutsomplia G, Lambrou G. Resistance mechanisms in the radiation therapy of osteosarcoma: a brief review. *J Res Pract Muscoloskeletal Syst.* (2020) 4:15–9.

31. Geller DS, Morris J, Revskaya E, Kahn M, Zhang W, Piperdi S, et al. Targeted therapy of osteosarcoma with radiolabeled monoclonal antibody to an insulin-like growth factor-2 receptor (IGF2R). *Nucl Med Biol.* (2016) 43:812–7. doi: 10.1016/j.nucmedbio.2016.07.008

32. Westrøm S, Bønsdorff TB, Abbas N, Bruland ØS, Jonasdottir TJ, Mælandsmo GM, et al. Evaluation of CD146 as target for radioimmunotherapy against osteosarcoma. *PLoS One.* (2016) 11:e0165382. doi: 10.1371/journal.pone.0165382

33. Larsen RH, Bruland OS, Hoff P, Alstad J, Lindmo T, Rofstad EK. Inactivation of human osteosarcoma cells in vitro by 211At-TP-3 monoclonal antibody: comparison with astatine-211-labeled bovine serum albumin, free astatine-211 and external-beam X rays. *Radiat Res.* (1994) 139:178–84.

34. Larsen RH, Bruland OS, Hoff P, Alstad J, Rofstad EK. Analysis of the therapeutic gain in the treatment of human osteosarcoma microcolonies in vitro with 211At-labelled monoclonal antibody. *Br J Cancer.* (1994) 69:1000–5. doi: 10.1038/bjc.1994.196

35. Larsen RH, Bruland OS. Intratumour injection of immunoglobulins labelled with the alpha-particle emitter 211At: analyses of tumour retention, microdistribution and growth delay. *Br J Cancer.* (1998) 77:1115–22. doi: 10.1038/bjc.1998.185

36. Aurlien E, Larsen RH, Akabani G, Olsen DR, Zalutsky MR, Bruland OS. Exposure of human osteosarcoma and bone marrow cells to tumour-targeted alpha-particles and gamma-irradiation: analysis of cell survival and microdosimetry. *Int J Radiat Biol.* (2000) 76:1129–41. doi: 10.1080/09553000050111604

37. Li HK, Hasegawa S, Nakajima NI, Morokoshi Y, Minegishi K, Nagatsu K. Targeted cancer cell ablation in mice by an α-particle-emitting astatine-211-labeled antibody against major histocompatibility complex class I chain-related protein A and B. *Biochem Biophys Res Commun.* (2018) 506:1078–84. doi: 10.1016/j.bbrc.2018.10.157

38. Karkare S, Allen KJH, Jiao R, Malo ME, Dawicki W, Helal M, et al. Detection and targeting insulin growth factor receptor type 2 (IGF2R) in osteosarcoma PDX in mouse models and in canine osteosarcoma tumors. *Sci Rep.* (2019) 9:11476. doi: 10.1038/s41598-019-47808-y

39. Martins CD, Kramer-Marek G, Oyen WJG. Radioimmunotherapy for delivery of cytotoxic radioisotopes: current status and challenges. *Expert Opin Drug Deliv.* (2018) 15:185–96. doi: 10.1080/17425247.2018.1378180

40. Bruland O, Thora JJ, Darrell FR, Roy LH. Radium-223: from radiochemical development to clinical applications in targeted cancer therapy. *Curr Radiopharm.* (2008) 1:203–8.

41. Bruland ØS, Nilssen S, Fisher DR, Larsen RH. High-linear energy transfer irradiation targeted to skeletal metastases by the alpha-emitter 223Ra: adjuvant or alternative to conventional modalities? *Clin Cancer Res.* (2006) 12(20 Pt 2):6250s–7s.

42. Parker C, Nilsson S, Heinrich D, Helle SI, O'Sullivan JM, Fosså SD, et al. Alpha emitter radium-223 and survival in metastatic prostate cancer. *N Engl J Med.* (2013) 369:213–23.

43. Anderson PM, Subbiah V, Rohren E. Bone-seeking radiopharmaceuticals as targeted agents of osteosarcoma: samarium-153-EDTMP and radium-223. *Adv Exp Med Biol.* (2014) 804:291–304. doi: 10.1007/978-3-319-04843-7_16

44. Anderson PM. Radiopharmaceuticals for Treatment of Osteosarcoma. *Adv Exp Med Biol* (2020) 1257:45–53.

45. Anderson PM, Scott J, Parsai S, Zahler S, Worley S, Shrikanthan S, et al. 223-Radium for metastatic osteosarcoma: combination therapy with other agents and external beam radiotherapy. *ESMO Open.* (2020) 5:e000635. doi: 10.1136/esmoopen-2019-000635

46. Subbiah V, Anderson P, Rohren E. Alpha emitter radium 223 in high-risk osteosarcoma: first clinical evidence of response and blood-brain barrier penetration. *JAMA Oncol.* (2015) 1:253–5. doi: 10.1001/jamaoncol.2014.289

47. Larsen RH, Sciencons AS. *Radiopharmaceutical Solutions with Advantageous Properties.* U.S. Patent No US 9,433,690 B1. (2016). Available online at: https://patents.google.com/patent/US9433690B1/en

48. Nelson BJB, Andersson JD, Wuest F. Targeted alpha therapy: progress in radionuclide production, radiochemistry, and applications. *Pharmaceutics.* (2020) 13:49. doi: 10.3390/pharmaceutics13010049

49. Kokov KV, Egorova BV, German MN, Klabukov ID, Krasheninnikov ME, Larkin-Kondrov AA, et al. (212)Pb: production approaches and targeted therapy applications. *Pharmaceutics.* (2022) 14:189. doi: 10.3390/pharmaceutics14010189

50. Chappell LL, Dadachova E, Milenic DE, Garmestani K, Wu C, Brechbiel MW. Synthesis, characterization, and evaluation of a novel bifunctional chelating agent for the lead isotopes 203Pb and 212Pb. *Nucl Med Biol.* (2000) 27:93–100. doi: 10.1016/s0969-8051(99)00086-4

51. Maaland AF, Saidi A, Torgue J, Heyerdahl H, Stallons TAR, Kolstad A, et al. Targeted alpha therapy for chronic lymphocytic leukaemia and non-Hodgkin's lymphoma with the anti-CD37 radioimmunoconjugate 212Pb-NNV003. *PLoS One.* (2020) 15:e0230526. doi: 10.1371/journal.pone.0230526

52. Stenberg VY, Larsen RH, Ma LW, Peng Q, Juzenas P, Bruland ØS, et al. Evaluation of the PSMA-binding ligand (212)Pb-NG001 in multicellular tumour spheroid and mouse models of prostate cancer. *Int J Mol Sci.* (2021) 22:4815. doi: 10.3390/ijms22094815

53. Stenberg VY, Tornes AJK, Nilsen HR, Revheim ME, Bruland ØS, Larsen RH, et al. Factors influencing the therapeutic efficacy of the PSMA targeting radioligand (212)Pb-NG001. *Cancers.* (2022) 14:2784. doi: 10.3390/cancers14112784

54. Kasten BB, Gangrade A, Kim H, Fan J, Ferrone S, Ferrone CR, et al. (212)Pb-labeled B7-H3-targeting antibody for pancreatic cancer therapy in mouse models. *Nucl Med Biol.* (2018) 58:67–73.

55. Meredith RF, Torgue JJ, Rozgaja TA, Banaga EP, Bunch PW, Alvarez RD, et al. Safety and outcome measures of first-in-human intraperitoneal α radioimmunotherapy with 212Pb-TCMC-trastuzumab. *Am J Clin Oncol.* (2018) 41:716–21. doi: 10.1097/COC.0000000000000353

56. Milenic DE, Baidoo KE, Kim YS, Brechbiel MW. Evaluation of cetuximab as a candidate for targeted α-particle radiation therapy of HER1-positive disseminated intraperitoneal disease. *MAbs.* (2015) 7:255–64. doi: 10.4161/19420862.2014.985160

57. Tan Z, Chen P, Schneider N, Glover S, Cui L, Torgue J, et al. Significant systemic therapeutic effects of high-LET immunoradiation by 212Pb-trastuzumab against prostatic tumors of androgen-independent human prostate cancer in mice. *Int J Oncol.* (2012) 40:1881–8. doi: 10.3892/ijo.2012.1357

58. Dos Santos JC, Schäfer M, Bauder-Wüst U, Lehnert W, Leotta K, Morgenstern A, et al. Development and dosimetry of (203)Pb/(212)Pb-labelled PSMA ligands: bringing "the lead" into PSMA-targeted alpha therapy? *Eur J Nucl Med Mol Imaging.* (2019) 46:1081–91. doi: 10.1007/s00259-018-4220-z

59. Corroyer-Dulmont A, Valable S, Falzone N, Frelin-Labalme AM, Tietz O, Toutain J, et al. VCAM-1 targeted alpha-particle therapy for early brain metastases. *Neuro Oncol.* (2020) 22:357–68.

60. Quelven I, Monteil J, Sage M, Saidi A, Mounier J, Bayout A, et al. (212)Pb α-radioimmunotherapy targeting CD38 in multiple myeloma: a preclinical study. *J Nucl Med.* (2020) 61:1058–65. doi: 10.2967/jnumed.119.239491

61. Banerjee SR, Minn I, Kumar V, Josefsson A, Lisok A, Brummet M, et al. Preclinical evaluation of (203/212)Pb-labeled low-molecular-weight compounds for targeted radiopharmaceutical therapy of prostate cancer. *J Nucl Med.* (2020) 61:80–8. doi: 10.2967/jnumed.119.229393

62. Stenberg VY, Juzeniene A, Bruland ØS, Larsen RH. In situ generated 212Pb-PSMA ligand in a 224Ra-solution for dual targeting of prostate cancer sclerotic stroma and PSMA-positive cells. *Curr Radiopharm.* (2020) 13:130–41. doi: 10.2174/1874471013666200511000532

63. Juzeniene A, Bernoulli J, Suominen M, Halleen J, Larsen RH. Antitumor activity of novel bone-seeking, α-emitting (224)Ra-solution in a breast cancer skeletal metastases model. *Anticancer Res.* (2018) 38:1947–55. doi: 10.21873/anticanres.12432

64. Sutherland RM. Cell and environment interactions in tumor microregions: the multicell spheroid model. *Science.* (1988) 240:177–84.

65. Casey RC, Burleson KM, Skubitz KM, Pambuccian SE, Oegema TR Jr., Ruff LE, et al. Beta 1-integrins regulate the formation and adhesion of ovarian carcinoma multicellular spheroids. *Am J Pathol.* (2001) 159:2071–80. doi: 10.1016/s0002-9440(10)63058-1

66. Nunes AS, Barros AS, Costa EC, Moreira AF, Correia IJ. 3D tumor spheroids as in vitro models to mimic in vivo human solid tumors resistance to therapeutic drugs. *Biotechnol Bioeng.* (2019) 116:206–26.

67. Nath S, Devi GR. Three-dimensional culture systems in cancer research: focus on tumor spheroid model. *Pharmacol Ther.* (2016) 163:94–108.

68. Edmondson R, Broglie JJ, Adcock AF, Yang L. Three-dimensional cell culture systems and their applications in drug discovery and cell-based biosensors. *Assay Drug Dev Technol.* (2014) 12:207–18.

69. Boyd M, Broglie JJ, Adcock AF, Yang L. Radiation quality-dependent bystander effects elicited by targeted radionuclides. *J Pharm Pharmacol.* (2008) 60:951–8. doi: 10.1211/jpp.60.8.0002

70. Chow T, Wutami I, Lucarelli E, Choong PF, Duchi S, Di Bella C. Creating in vitro three-dimensional tumor models: a guide for the biofabrication of a primary osteosarcoma model. *Tissue Eng Part B Rev.* (2021) 27:514–29. doi: 10.1089/ten.TEB.2020.0254

71. Mueller-Klieser W, Freyer JP, Sutherland RM. Influence of glucose and oxygen supply conditions on the oxygenation of multicellular spheroids. *Br J Cancer.* (1986) 53:345–53.

72. Jiang Y, Pjesivac-Grbovic J, Cantrell C, Freyer JP. A multiscale model for avascular tumor growth. *Biophys J.* (2005) 89:3884–94.

73. Fodstad O, Brøgger A, Bruland O, Solheim OP, Nesland JM, Pihl A. Characteristics of a cell line established from a patient with multiple osteosarcoma, appearing 13 years after treatment for bilateral retinoblastoma. *Int J Cancer.* (1986) 38:33–40. doi: 10.1002/ijc.2910380107

74. Westrøm S, Generalov R, Bønsdorff TB, Larsen RH. Preparation of (212)Pb-labeled monoclonal antibody using a novel (224)Ra-based generator solution. *Nucl Med Biol.* (2017) 51:1–9. doi: 10.1016/j.nucmedbio.2017.04.005

75. Li, RG, Stenberg VY, Larsen RH. A novel experimental generator for production of high purity lead-212 for use in radiopharmaceuticals. *J Nucl Med.* (2022):jnumed.122.264009. doi: 10.2967/jnumed.122.264009

76. Napoli E, Stenberg VY, Juzeniene A, Hjellum GE, Bruland ØS, Larsen RH. Calibration of sodium iodide detectors and reentrant ionization chambers for (212)Pb activity in different geometries by HPGe activity determined samples. *Appl Radiat Isot.* (2020) 166:109362. doi: 10.1016/j.apradiso.2020.109362

77. Larsen RH, Sciencons AS. *Production of Highly Purified 212Pb.* Patent WO 2021/110950 A1. (2021). Available online at: https://publications.gc.ca/collections/collection_2022

78. Carlsson J, Yuhas JM. Liquid-overlay culture of cellular spheroids. *Recent Results Cancer Res.* (1984) 95:1–23.

79. Ivascu A, Kubbies M. Rapid generation of single-tumor spheroids for high-throughput cell function and toxicity analysis. *J Biomol Screen.* (2006) 11:922–32. doi: 10.1177/1087057106292763

80. Grignani G, Palmerini E, Ferraresi V, D'Ambrosio L, Bertulli R, Asaftei SD, et al. Sorafenib and everolimus for patients with unresectable high-grade osteosarcoma progressing after standard treatment: a non-randomised phase 2 clinical trial. *Lancet Oncol.* (2015) 16:98–107. doi: 10.1016/S1470-2045(14)71136-2

81. Marchandet L, Lallier M, Charrier C, Baud'huin M, Ory B, Lamoureux F. Mechanisms of resistance to conventional therapies for osteosarcoma. *Cancers.* (2021) 13:683.

82. Bielack S, Jürgens H, Jundt G, Kevric M, Kühne T, Reichardt P, et al. Osteosarcoma: the COSS experience. *Cancer Treat Res.* (2009) 152:289–308.

83. Khanna C, Wan X, Bose S, Cassaday R, Olomu O, Mendoza A, et al. The membrane-cytoskeleton linker ezrin is necessary for osteosarcoma metastasis. *Nat Med.* (2004) 10:182–6.

84. Mansi JL, Gogas H, Bliss JM, Gazet JC, Berger U, Coombes RC. Outcome of primary-breast-cancer patients with micrometastases: a long-term follow-up study. *Lancet.* (1999) 354:197–202.

85. Pantel K, Cote RJ, Fodstad O. Detection and clinical importance of micrometastatic disease. *J Natl Cancer Inst.* (1999) 91:1113–24.

86. Wiedswang G, Borgen E, Kåresen R, Kvalheim G, Nesland JM, Qvist H, et al. Detection of isolated tumor cells in bone marrow is an independent prognostic factor in breast cancer. *J Clin Oncol.* (2003) 21:3469–78.

87. Brunsvig PF, Flatmark K, Aamdal S, Høifødt H, Le H, Jakobsen E, et al. Bone marrow micrometastases in advanced stage non-small cell lung carcinoma patients. *Lung Cancer.* (2008) 61:170–6.

88. Braun S, Vogl FD, Naume B, Janni W, Osborne MP, Coombes RC, et al. A pooled analysis of bone marrow micrometastasis in breast cancer. *N Engl J Med.* (2005) 353:793–802.

89. Däster S, Amatruda N, Calabrese D, Ivanek R, Turrini E, Droeser RA, et al. Induction of hypoxia and necrosis in multicellular tumor spheroids is associated with resistance to chemotherapy treatment. *Oncotarget.* (2017) 8:1725–36.

90. Perche F, Torchilin VP. Cancer cell spheroids as a model to evaluate chemotherapy protocols. *Cancer Biol Ther.* (2012) 13:1205–13. doi: 10.4161/cbt.21353

91. Carretta A. Clinical value of nodal micrometastases in patients with non-small cell lung cancer: time for reconsideration? *J Thorac Dis.* (2016) 8:E1755–8. doi: 10.21037/jtd.2016.12.83

92. Larsen RH, Hoff P, Vergote IB, Bruland OS, Aas M, De Vos L, et al. Alpha-particle radiotherapy with 211At-labeled monodisperse polymer particles, 211At-labeled IgG proteins, and free 211At in a murine intraperitoneal tumor model. *Gynecol Oncol.* (1995) 57:9–15. doi: 10.1006/gyno.1995.1093

93. Anderson PM, Meyers DE, Hasz DE, Covalcuic K, Saltzman D, Khanna C, et al. In vitro and in vivo cytotoxicity of an anti-osteosarcoma immunotoxin containing pokeweed antiviral protein. *Cancer Res.* (1995) 55:1321–7.

94. Ek O, Waurzyniak B, Myers DE, Uckun FM. Antitumor activity of TP3(anti-p80)-pokeweed antiviral protein immunotoxin in hamster cheek pouch and severe combined immunodeficient mouse xenograft models of human osteosarcoma. *Clin Cancer Res.* (1998) 4:1641–7.

95. Onda M, Bruland ØS, Pastan I. TP-3 immunotoxins improve antitumor activity in mice with osteosarcoma. *Clin Orthop Relat Res.* (2005):142–8. [Epub ahead of print].

96. Kim JS, Jun SY, Kim YS. Critical issues in the development of immunotoxins for anticancer therapy. *J Pharm Sci.* (2020) 109:104–15.

97. Ballangrud AM, Yang WH, Charlton DE, McDevitt MR, Hamacher KA, Panageas KS, et al. Response of LNCaP spheroids after treatment with an alpha-particle emitter (213Bi)-labeled anti-prostate-specific membrane antigen antibody (J591). *Cancer Res.* (2001) 61:2008–14.

98. Hjelstuen MH, Rasch-Halvorsen K, Brekken C, Bruland O, de L, Davies C. Penetration and binding of monoclonal antibody in human osteosarcoma multicell spheroids. Comparison of confocal laser scanning microscopy and autoradiography. *Acta Oncol.* (1996) 35:273–9. doi: 10.3109/02841869609101641

99. Nair AB, Jacob S. A simple practice guide for dose conversion between animals and human. *J Basic Clin Pharm.* (2016) 7:27–31. doi: 10.4103/0976-0105.177703

100. Blair HC, Larrouture QC, Li Y, Lin H, Beer-Stoltz D, Liu L, et al. Osteoblast differentiation and bone matrix formation in vivo and in vitro. *Tissue Eng Part B Rev.* (2017) 23:268–80.

101. Jacques C, Renema N, Ory B, Walkley CR, Grigoriadis AE, Heymann D. Murine models of bone sarcomas. *Methods Mol Biol.* (2019) 1914:331–42.

102. Suominen MI, Rissanen JP, Käkönen R, Fagerlund KM, Alhoniemi E, Mumberg D, et al. Survival benefit with radium-223 dichloride in a mouse model of breast cancer bone metastasis. *J Natl Cancer Inst.* (2013) 105:908–16. doi: 10.1093/jnci/djt116